

Nano - carbide precipitation strengthening in a newly developed HSLA steel

(奈米級碳化物析出強化之高強度低合金鋼)

C. Y. Chen (陳志遠)^a, J. R. Yang (楊哲人)

Department of Materials Science and Engineering, National Taiwan University, Taipei ,
Taiwan

^ad92527002@ntu.edu.tw

Newly-developed HSLA steels have been claimed to possess an extremely high strength due to precipitation hardening of nano-sized carbides. Transmission electron microscopy and microhardness measurements of individual ferrite grains were employed to investigate the state of precipitation in an experiment HSLA steel. It is found that the isothermal aging temperature would influence the precipitation state in the ferrite. Carbides, which precipitated between α/γ interface and within supersaturated α matrix, are the main sources for the strengthening in this steel. The higher isothermal aging temperature would reduce the ledge migration velocity and lead to large-sized carbides with a wider band spacing. However, $\gamma \rightarrow \alpha$ phase transformation in the low isothermal aging temperature could accelerate ledge migration and inhibit micro-alloying carbides to nucleate as well as growth. The micro-alloying elements can retain in matrix, and thereby promote the supersaturated precipitates in the ferrite matrix in the following isothermal aging process. The nano-scaled size of these supersaturated carbides is associated with low temperature diffusivity of micro alloying elements.

Keywords: newly-developed HSLA steel, TEM, Interface precipitation, supersaturated precipitation.

1. Introduction

Developing high-strength steels for automobile application is an effective way to decrease vehicle weight. These steels derive their high strength from a combination of mechanisms including solid solution, grain size, dislocation and precipitation hardening. Among these strengthening methods, nano-sized precipitates could increase steel strength effectively ⁽¹⁻⁵⁾. Gladman had pointed out that maximum precipitation strengthening happens with carbides of about 3-5 nm ⁽⁶⁾. However, according to previous studies ⁽⁷⁾, precipitates are expected to be formed at different stage of processing of the steel on the basis of thermodynamic and kinetic considerations. For example: (1) coarse precipitates (>100nm) could form at high temperature in the austenite region (e.g. TiN). (2) medium size precipitates (>20~50nm) produced by strain induced precipitation after rolling in the non-recrystallized region. (3) fine precipitates (20~50nm) could form in the high temperature ferrite region. (4) very fine precipitate (<5nm) form during coiling after rolling. Therefore most microalloying elements (Ti, V, Nb) would be exhausted in the soaking and rolling process which would reduce the quantity of nano-sized precipitation in the low temperature ferrite region.

Interface precipitation of fine carbides during austenite to ferrite phase transformation and carbides precipitation form supersaturated ferrite matrix are generally recognized as two important mechanisms for strengthening of hot-rolled steel ^(3, 8-11). However, it is also found that interface precipitation can only occur in some of the ferrite grains not in all ones and the sizes of interface precipitation carbides also differ largely ⁽¹²⁻¹³⁾. So that the characterization of non-uniformly distribution of interface precipitates would affect the strength of ferritic grains greatly. On the other hand it is generally regarded that the supersaturated precipitation carbides would form at dislocations in very low temperatures range (<600°C) ⁽¹⁴⁾, which would likely lead to precipitation in the Widmanstätten ferrite which would not benefit for the toughness of the steels. However, the mechanism of interface precipitation and supersaturated precipitation in the low temperature has still not been reliably established.

The present work is to provide insight into the precipitation behavior of a state-of-the-art HSLA steel containing microalloying additions of Ti and Mo. The evolution of precipitates in Ti-Mo microalloyed steels at different isothermal temperatures for different holding times are examined in terms of their morphology, size and crystallography based on both TEM observation and microhardness measurement.

2. Experimental procedure

The chemical composition of the steel used in the present work was composed of 0.1C-0.1Si-1.5Mn-0.01P-0.004S-0.2Ti-0.2Mo (wt %). Dilatometer specimens with 6mm length and 3mm diameter were machined from the half positions of the original steel plate along the rolling direction. All the heat treatment processes were carried out on a Dilatronic III RDP dilatometer of Theta Industries, Inc. The dilatometer was interfaced with a computer work station (PDP 11/55 central processor) for analyzing the resulting data. A software package (provide by Theta Industries) can allow a flexible control to execute the isothermal transformation experiments. A vacuum of 10^{-5} torr was maintained to protect specimens from oxidation during the process. The heat treatment process is shown schematically in Fig. 1. The specimens were heated at the rate of $10^{\circ}\text{C}/\text{sec}$ from the room temperature to 1200°C and kept at this temperature for 3 minutes to dissolve all the carbide particles. After austenitizing at 1200°C , the specimens were directly cooled to 700°C as well as 625°C at a cooling rate of $20^{\circ}\text{C}/\text{sec}$ and kept at this temperature for 5 min, 10min, and 60min respectively. After isothermal transformation was completed for different time intervals, the specimens were then directly quenched to room temperature.

The samples for optical metallography, prepared from dilatometer specimen, were mechanical polished and then etched in 2% nital solution. Transformation electron microscopy (TEM) specimens were prepared from 0.25mm thick discs sliced from dilatometer specimen. The discs were thinned to 0.07mm by abrasion on SiC papers and twin jet electropolished using a mixture of 5% perchloric acid, 25% glycerol, and 70% ethanol at the temperature -5°C to -10°C at 45V etching potential. They were examined using JEOL-2000EX transmission electron microscopes operated at 200kv. Futhermore, the composition analyses of nano precipitates were examined using a FEG-TEM Tecnai F30 equipped with nano probe EDS. The microhardness of the dilatometric specimens were determined with a Vickers hardness tester using a 100g load.

3. Result and discussion

Figs 2(a)-(f) show typical microstructure of specimens after different isothermal aging temperature and time. It can be seen from these microstructures that the amount of ferrite increases with increasing isothermal aging time at 625°C and 725°C respectively. The gray area in these microstructure is martensite which resulted from untransformed austenite during quenching process. After long time (60 min) aging at 625°C , the microstructure is composed of ferrite and pearlite. However, martensite still could be seen after the same holding time at 725°C . The difference between

microstructures obtained at 625 and 725°C is related to the nature of equilibrium quantity of phases at various temperatures, i.e. low isothermal aging temperature could get more ferrite.

The microhardness test result is shown in Fig.3 (a). The hardness of steel isothermally holding at 625°C would increase with time. However, the trend is opposite for high temperature aging. When aging time reaches 60min, values of Vickers hardness are 320 (625°C) and 200 (725°C) respectively. Because the hardness of ferrite reflects mainly the state of precipitation in the grain, it indicates that steel isothermally aging at 625°C should get high volume fraction of tiny precipitates in the ferrite matrix. Fig.3 (b)-(e) shows the microhardness distribution of the steel at various temperatures for different aging times. It could be seen that the distribution of microhardness holds a normal distribution. However, it should be noted that the microhardness distribution is wider for short isothermal aging time at low and high aging temperatures. This non-uniformly distribution of microhardness is consistent with the early report ⁽¹³⁾, and could be associated with the state of precipitation in the ferrite. As can be seen from Fig. 4, the carbide precipitates in the ferrite matrix at 625°C and 725°C for 60 min aging treatments appear to be two different modes of precipitation: interface precipitation and supersaturated precipitation. The sizes of these carbides formed at low and high temperature are about 4~6 nm and 15~ 20 nm respectively. As pointed by Gladman ⁽⁶⁾, the maximum strengthening occurs with particles of about 5 nm. The nano-sized carbides (4~6 nm) are expected to be the main contributor for high hardness at low temperature.

The orientation relationship between carbides and ferrite matrix is also different for interface precipitation and supersaturated precipitation. The KS relationship between interface precipitation carbides and ferrite matrix had been reported in many literatures ⁽¹⁵⁻¹⁷⁾. According to our previous research ⁽¹⁸⁾, interface precipitation carbides could also adapt NW relationship with ferrite matrix. Interface precipitation carbides nucleated at the austenite region of the ledge would have a cube to cube relationship with matrix. After ledge sweeping and completing austenite to ferrite phase transformation, interface precipitation carbides should inherit the orientation relationship between the former austenite and ferrite. Consequently, the carbides formed by interface precipitation mechanism should exhibit NW relationship with ferrite matrix. That is $(110)_\alpha // (111)_{MC}$, $[001]_\alpha // [\bar{1}0\bar{1}]_{MC}$. Because KS and NW relationship between austenite and ferrite generally occur in the low energy interfaces with a high degree of coherency, it is reasonable to get NW relationship between interface precipitation carbides and ferrite matrix. Instead, supersaturated precipitates nucleate directly in the ferrite matrix and would obey BN relationship with ferrite matrix ⁽¹⁹⁾. That is $(001)_\alpha // (001)_{MC}$, $[010]_\alpha // [110]_{MC}$.

Based on the above results, an attempt of this work was to investigate the mechanism of nano-sized supersaturated carbides precipitation in the low aging temperature. It is generally agreed that the size of interface precipitation carbides is inversely proportional to the ledge mobility^(3, 20-21). Low isothermal aging temperature would get tiny interface precipitation carbides and accelerate $\gamma \rightarrow \alpha$ phase transformation by large driving force, which means most ferrite grains could form in the very short time and lead to higher ledge mobility. When the mobility of the ledge is fast, interface precipitation carbides could not nucleate and growth, which would result microalloying elements remaining in the ferrite matrix. Since the solubility of these micro-alloying carbides in ferrite are at least an order of magnitude smaller than in austenite, these supersaturated microalloying elements would precipitate in the following aging process. These carbides are called supersaturated carbides, and the sizes of these carbides depend on the isothermal aging temperature. When aging temperature is low, supersaturated precipitate carbides would attain nano-sized (~5nm) and disperse uniformly in the ferrite matrix. Consequently, a lot of nano-sized carbides in the ferrite matrix would improve the strength of the steel.

According to previous investigation^(22, 23), the thickening rate of allotriomorphic ferrite should follow parabolic growth law, i.e. that the thickness of allotriomorphic ferrite is proportional to $t^{1/2}$, where t is time. From the view point of one individual allotriomorphic ferrite growth event, it is obviously that thickening rate of allotriomorphic ferrite would very fast at the beginning of transformation and slow down at the end. It seems that the decrease in ferrite growth rate brings about the structure change from precipitation free allotriomorphic ferrite generation initially to the formation of ferrite accompanied by aligned carbide precipitation at the later stages of isothermal transformation. Therefore, the state of interface precipitation is not uniformly in one ferrite grain, which depends on the kinetic of austenite transformation into ferrite (i.e. ledge's mobility). This non-uniform state of precipitation carbides at the beginning of $\gamma \rightarrow \alpha$ phase transformation would lead to large discrepancy on microhardness of ferrite grains in the short aging time. However, most carbides would nucleate and growth after long time aging, which would cause a normal distribution of microhardness. Fig. 5 integrates the above explanation about the distribution of interface precipitation and supersaturated precipitation in the ferrite matrix at different temperatures. Thereby it could be illustrated that nano-sized carbides should be formed by larger ledge mobility, and low diffusivity of metal atoms.

Because austenite transformation into ferrite is a diffusional phase transformation, the amount of ferrite formation in isothermal aging should also depend on the aging temperature. When the aging temperature is close to the nose of

ferrite formation C-curve, the austenite transformation into ferrite would be completed in shortly time interval, which implies that the ledge mobility is too high to form interface precipitation carbides. Therefore the matrix with higher concentration of micro-alloying elements would form supersaturated precipitation in most of ferrite grains after aging treatment. The quantity of supersaturated precipitate is also influenced by the aging temperature. Since the solubility of carbides is lower in the low temperature, it should get more supersaturated precipitates in the low aging temperature. Consequently, considerable amount of carbides formed at 625°C could maintain nano-sized (4~5 nm) and achieve higher hardness with aging time. However, aging at 725°C would obtain large sized carbides (15~20 nm) and the hardness of the steel would drop with aging time.

4. Conclusion

From the results investigated in this study, it is clear that aging temperature would influence ferrite mechanical properties greatly. The major conclusions are drawn as follows:

1. Both of interface precipitation and supersaturated precipitation of carbides would appear in the same ferrite grain, which could affect the ferrite hardness effectively.
2. Low aging temperature could reduce microalloying elements diffusivity and brings about larger supersaturation of carbides, which would generate a lot of nano-sized carbides in the ferrite matrix to improve the strength of steel.

Reference

1. M. Charleux, W. J. Poole, M. Militzer and A. Deschamps, "Precipitation behavior and its effect on strengthening of an HSLA-Nb/Ti steel", *Metall. Mater. Trans. A*, 2001, Vol. 32A, pp.1635-1647.
2. T. Gladman, "Precipitation hardening in metals", *Mater. Sci. Technol.*, 1999, Vol. 15, pp. 30-36.
3. Y. Funakawa, T. Shiozaki, K. Tomita, T. Yamamoto and E. Maeda, "Development of high strength hot-rolled sheet steel consisting of ferrite and nanometer-sized carbides", *ISIJ Int.*, 2004, Vol. 44, pp. 1945-1951.
4. Miloslav Beres, Thomas E. Weirich, Klaus Hulka, and Joacchim Mayer, "TEM investigation of fine niobium precipitates in HSLA steel", *Steel research int.*, 2004, no.11, pp. 753-758.
5. Hai-Long Yi, Lin-Xiu Du, Guo-Dong Wang and Xiang- Hua Liu, "Development of a hot-rolled low carbon steel with high yield strength", *ISIJ Int.*, 2006, Vol. 46, pp.754-758.
6. T. Gladman, *The physical Metallurgy of Microalloyed Steels*, The institute of materials, 1997, P.54.
7. R. D. K. Misra, G. C. Weatherly, J. E. Hartmann, and A. J. Boucek, "Ultrahigh strength hot rolled microalloyed steels: microstructural aspects of development", *Mater. Sci. Technol.*, 201, Vol. 17, pp. 1119-1129.
8. H.-J. Kestenbach, "Dispersion hardening by niobium carbonitride precipitation in ferrite", *Mater. Sci Technol.*, 1997, Vol. 13, pp.731-739.
9. T. Sakuma and R. W. K. Honeycombe, "Microstructures of isothermally transformed Fe-Nb-C alloys", *Metal Sci.*, 1984, Vol. 18, pp. 449-454.
10. S. Freeman and R. W. K. Honeycombe, *Metal Sci.*, 1977, Vol. 11, pp. 59-64.
11. R. M. Brito and H.-J. Kestenbach, *J. Mater. Sci.*, 1981, Vol. 16, pp. 1257-1263.
12. Morrison WB, *J Iron Steel Inst.*, 1963, Vol. 201, pp. 317-325.
13. S. S. Campos, E. V. Morales, and H.-J. Kestenbach, "Detection of interface precipitation in microalloyed steels by microhardness measurements", *Materials Characterization*, 2004, 52, pp. 379-384.
14. G. M. Smith and R. W. K. Honeycombe, *Proc. 6th Int. CONF. on strength of Metals and Alloys*, 1982, p.407.
15. W. B. Lee, S. G. Hong, C. G. Park, and S. H. Park, "Carbide precipitation and high temperature strength of hot rolled high strength low alloy steels containing Nb and Mo", *Metall. Mater. Trans. A*, 2002, Vol. 33A, pp.1689-1698.
16. A. T. Davenport, L. C. Brossard, and R. E. Miner, *J. Met.*, 1975, Vol. 27(6), pp. 21-27.

17. A. J. DeArdo, "Niobium in modern steels", *Int. Mater. Rev.*, 2003, Vol. 48, No. 6, pp.371-402.
18. H. W. Yen, C. Y. Chen, C. Y. Huang, and J. R. Yang, "TEM investigation of nanometer-sized interface-precipitation in a Ti-containing HSLA steel", *The 3rd international conference on advanced structural steels*, Gyeongju, Korea, August 22-24, 2006, pp. 400-405.
19. R. G. Baker and J. Nutting, *ISI Special Report*, no. 64, 1959, p.1
20. R. W. K. Honeycombe, "Ferrite", *Metal Sci.*, 1980, pp. 201-214.
21. R. W. K. Honeycombe, "Transformation from austenite in alloy steels", *Metall. Mater. Trans. A*, 1976, Vol.7A, pp. 915-935.
22. W. J. Liu and J. J. Jonas, "Ti(CN) precipitation in microalloyed austenite during stress relaxation", *Mater. Trans. A*, 1988, Vol.19A, pp. 1415-1424.
23. C. Zener, *J. Appl. Phys.*, 1949, Vol. 20, pp. 950-953.

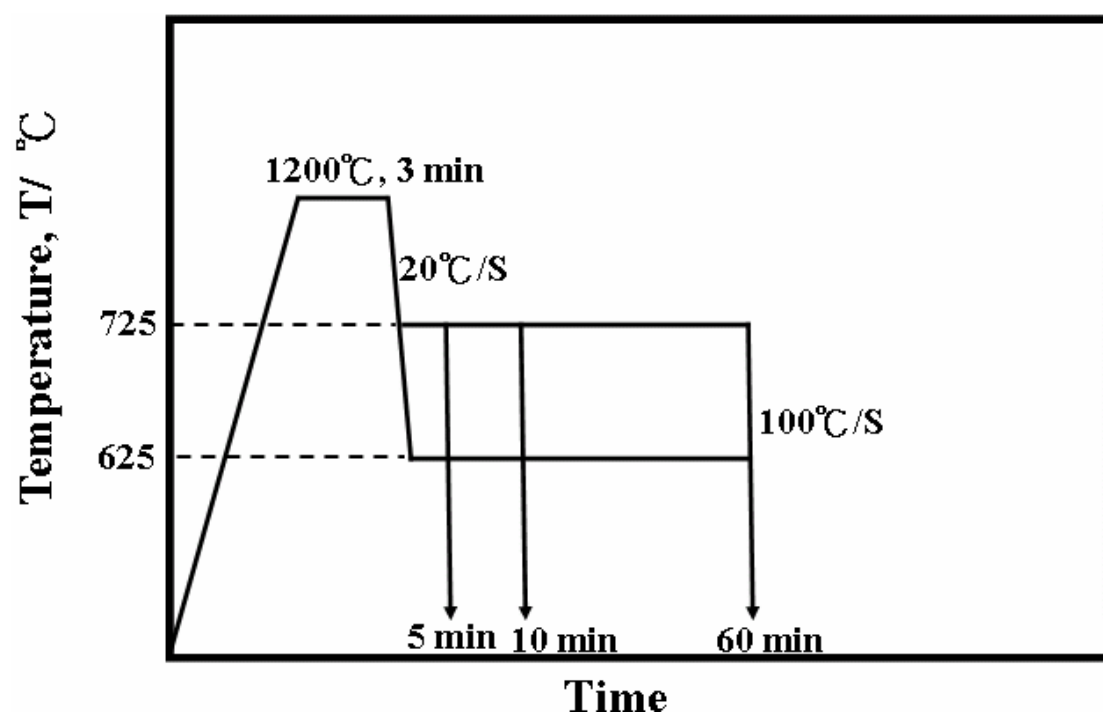


Fig. 1 Schematic diagram shows isothermal aging treatment procedure.

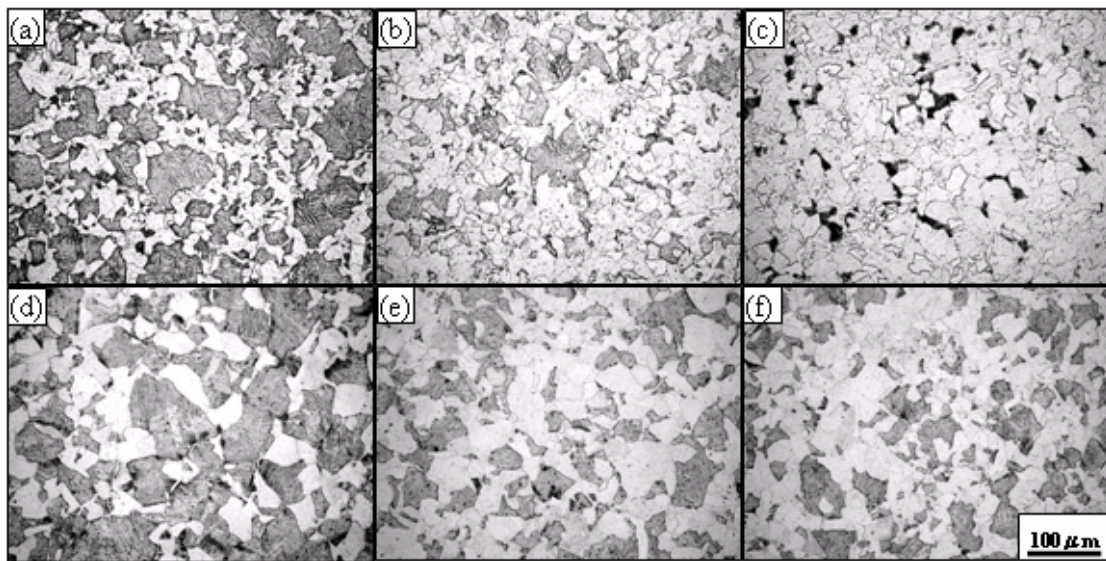


Fig. 2 Optical metallographs obtained from dilatometer specimens isothermal aging at 625°C for (a) 5min, (b) 10min, (c) 60min and 725°C for (d) 5min, (e) 10min, (f) 60min

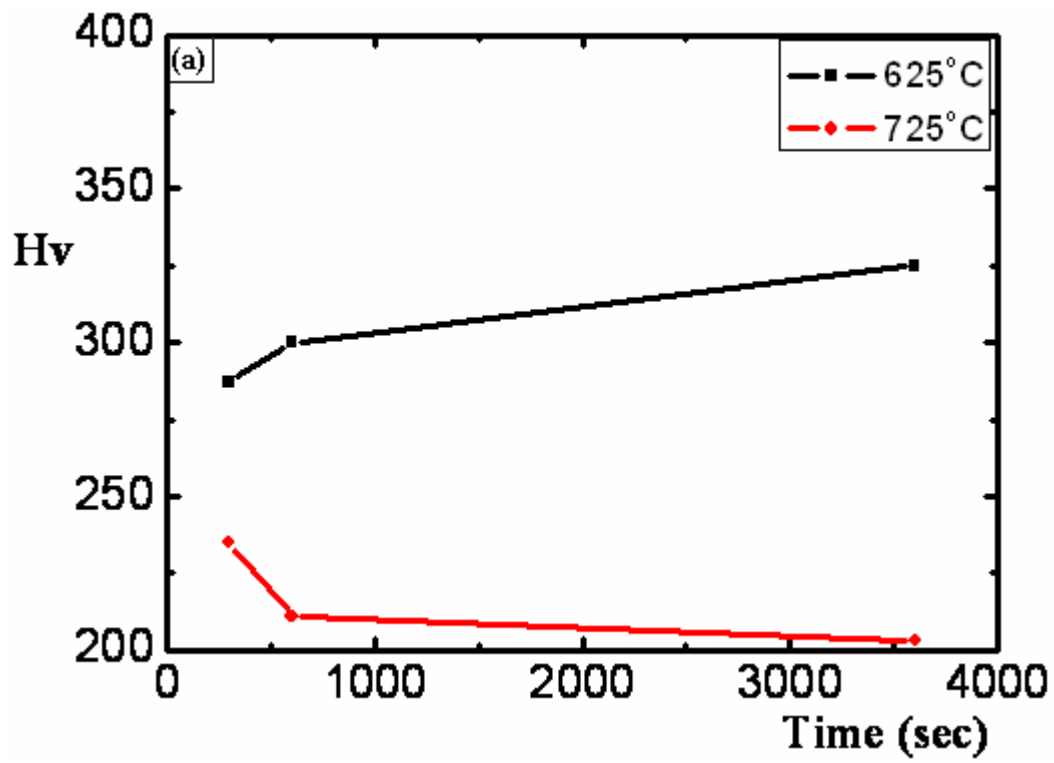
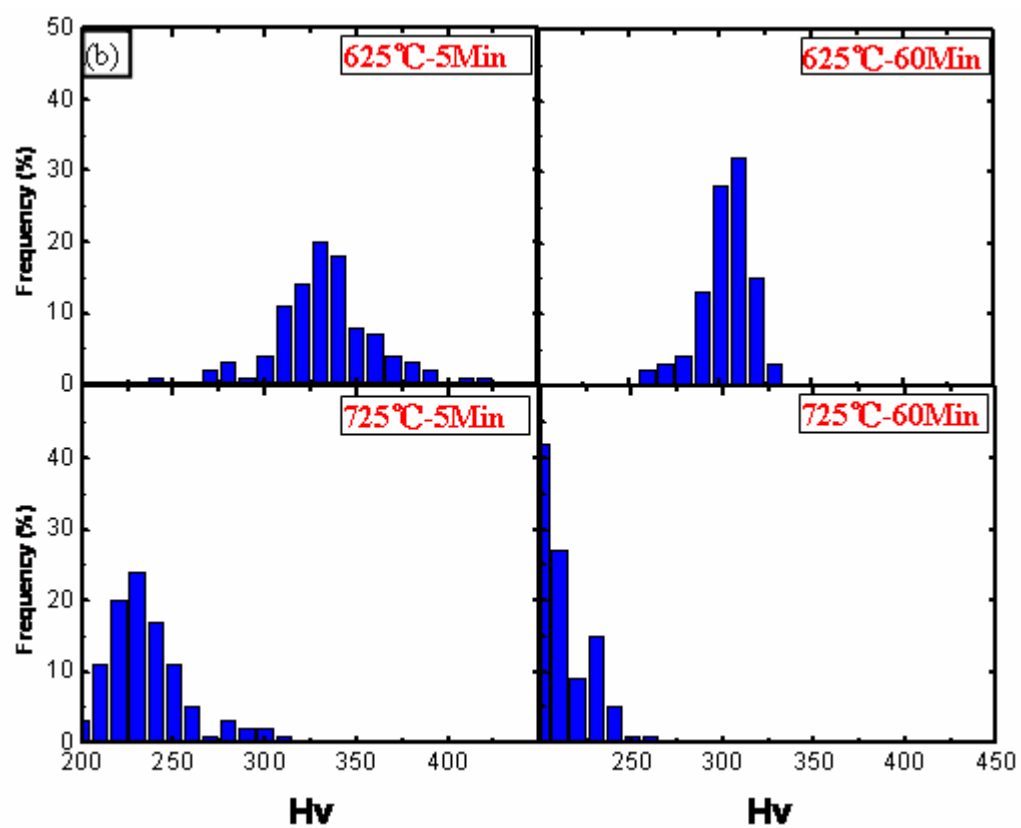


Fig. 3 (a) Effect of isothermal aging time and temperature on the microhardness of the steels

(b) microhardness distribution of steels at different isothermal aging temperatures and times.



(Fig. 3 continued)

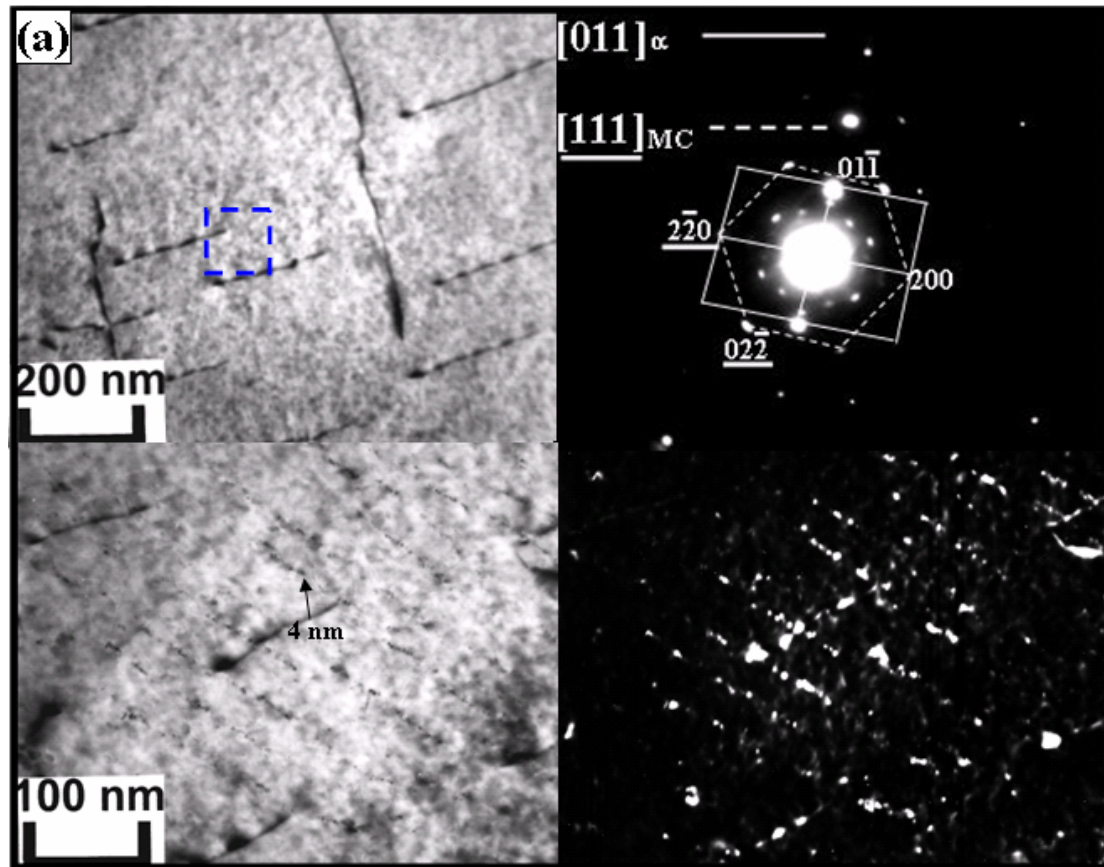
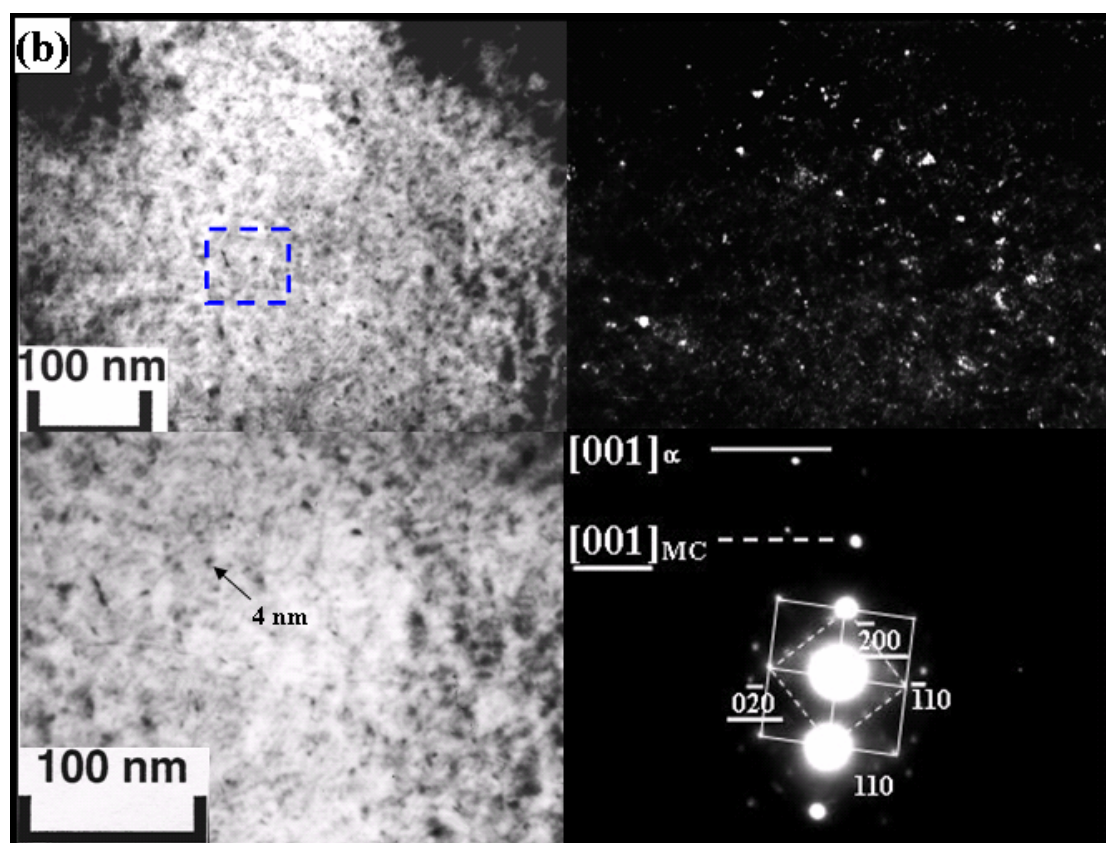
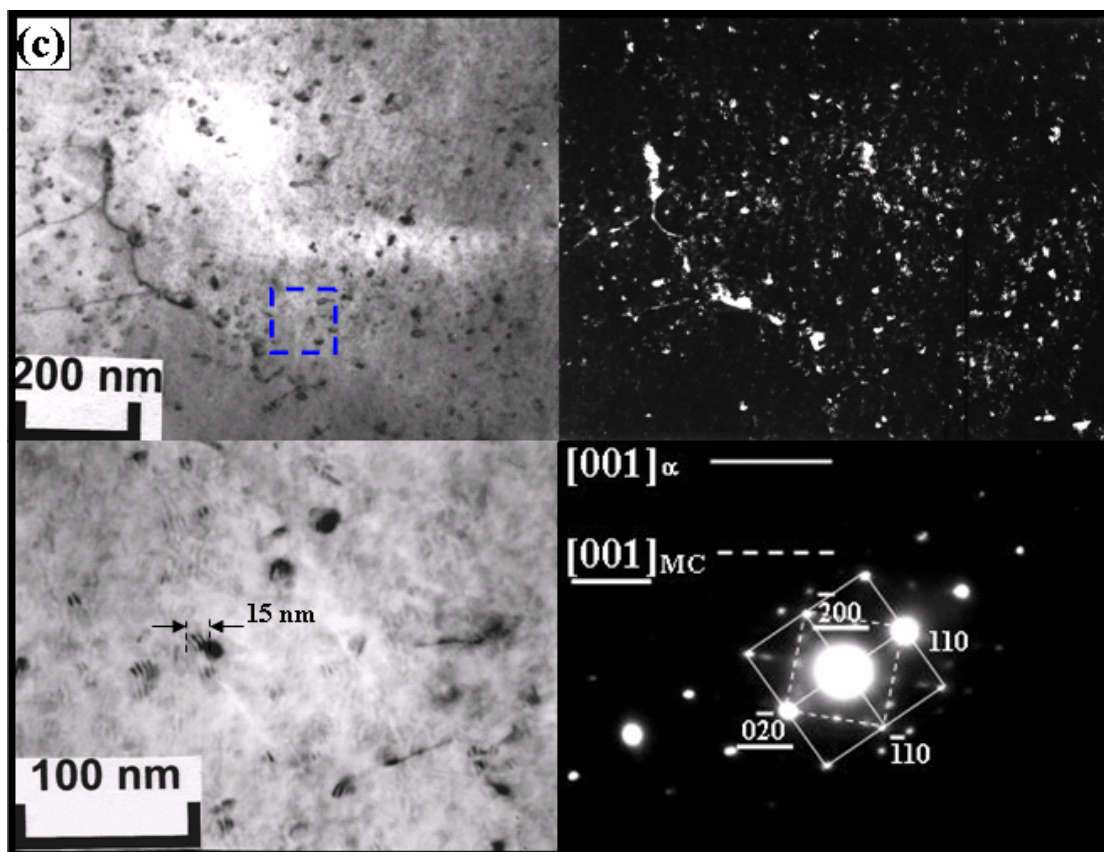


Fig. 4 Transmission electron micrographs show low magnification bright field image, centered dark field image, high magnification bright field image and corresponding diffraction pattern at different aging conditions. (a) 625°C 60 min interface precipitation, (b) 625°C 60 min supersaturated precipitation, (c) 725°C 60 min supersaturated precipitation, (d) 725°C 60 min interface precipitation.



(Fig. 4 continued)



(Fig. 4 continued)

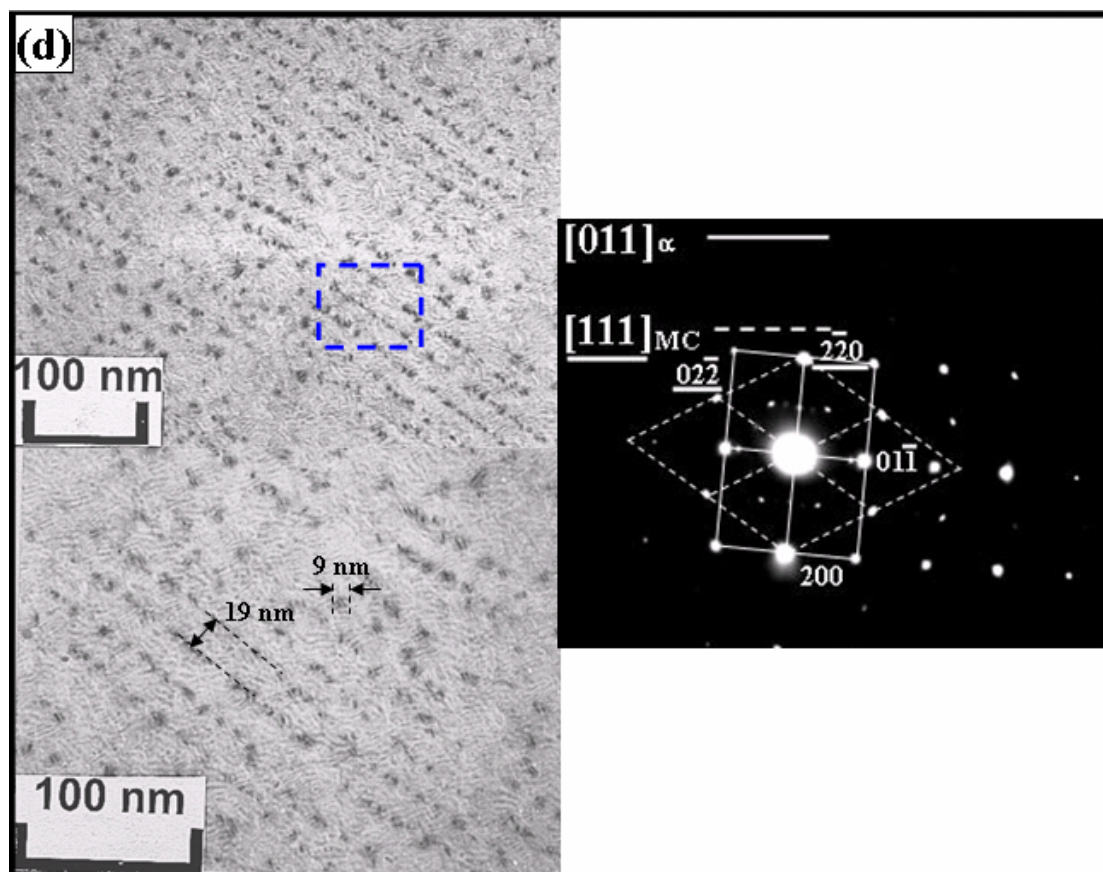


(Fig. 4 continued)

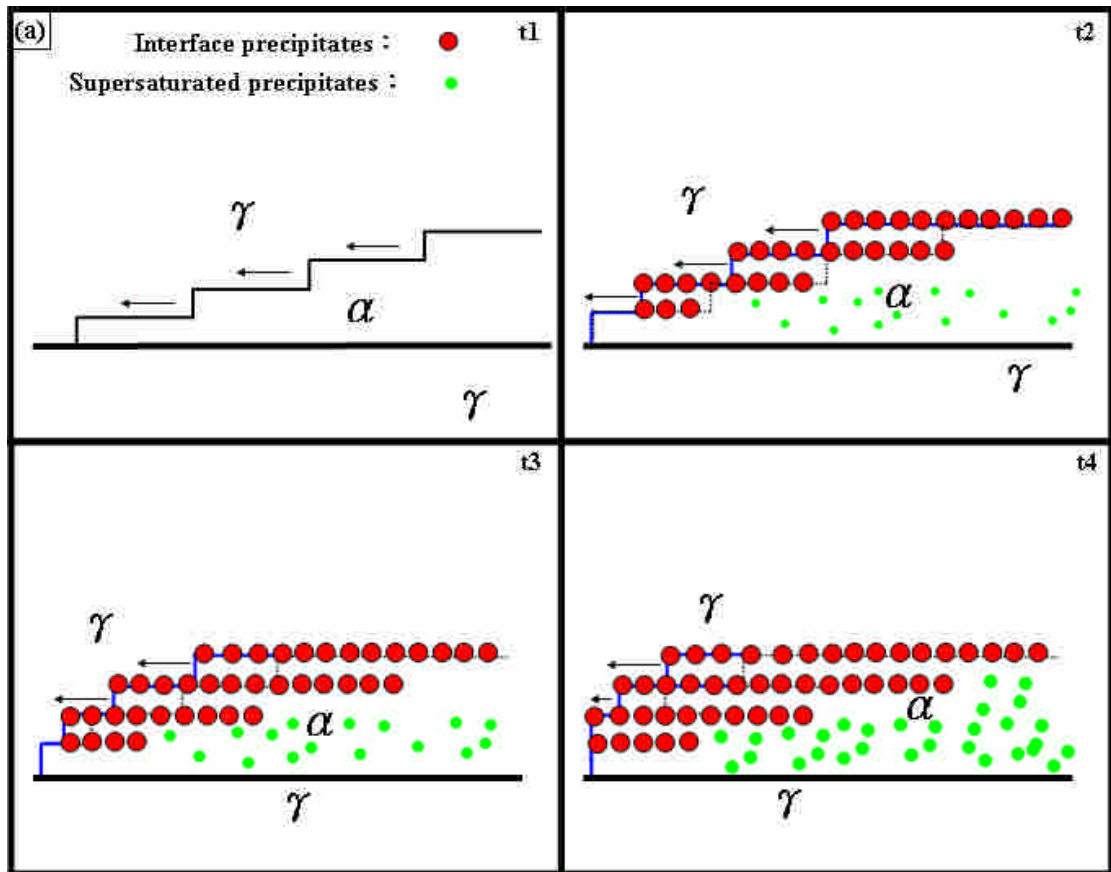
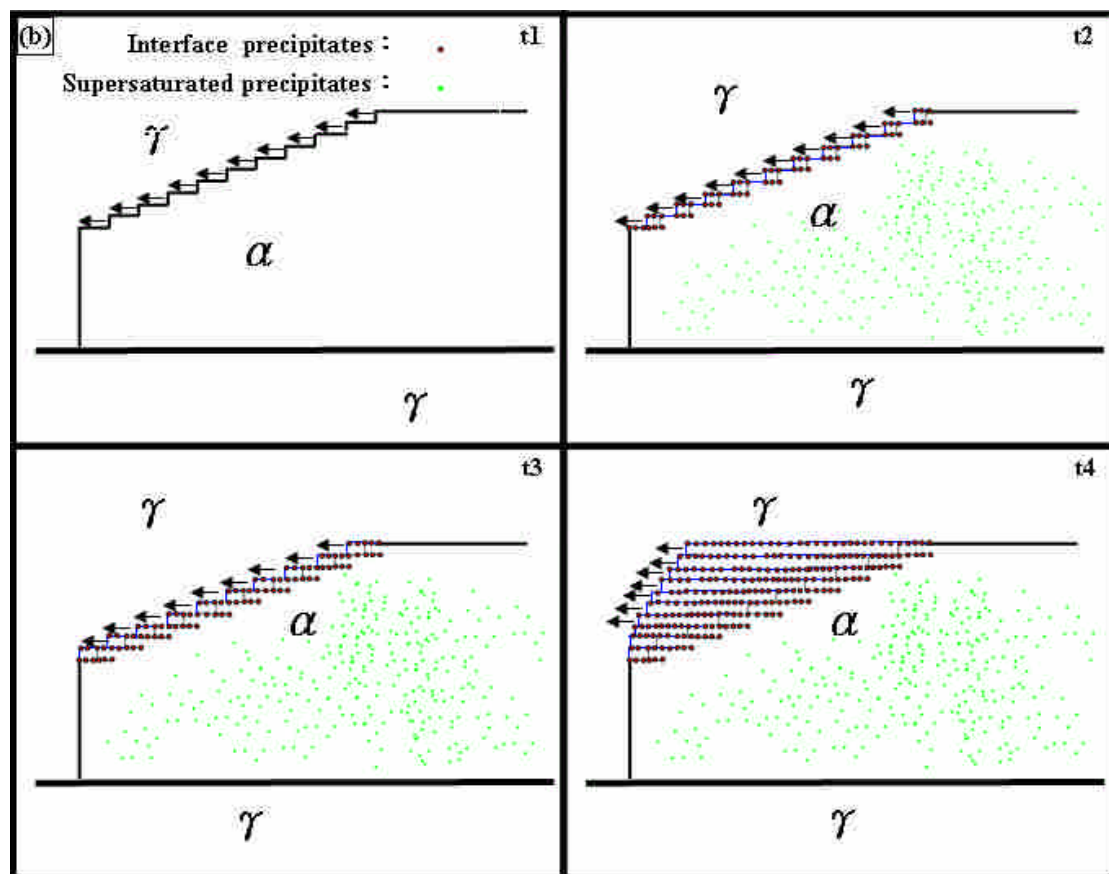


Fig. 5 Schematic illustrating the mechanism of precipitation in the ferrite matrix
 (a) high temperature isothermal aging, (b) low temperature isothermal aging,



(Fig. 5 continued)